FEBS Letters 582 (2008) 2309–2312

Domain versatility in plant AB-toxins: Evidence for a local, pH-dependent rearrangement in the 2γ lectin site of the mistletoe lectin by applying ligand derivatives and modelling

Marta Jiménez[a], Sabine André[b], Caterina Barillari[c], Antonio Romero[d], Didier Rognan[c], Hans-Joachim Gabius[b], Dolores Solís[a,*]

[a] *Instituto de Química Física Rocasolano, CSIC, Serrano 119, E-28006 Madrid, Spain*
[b] *Institut für Physiologische Chemie, Tierärztliche Fakultät, Ludwig-Maximilians-Universität, Veterinärstrasse 13, D-80539 München, Germany*
[c] *Laboratoire de Bioinformatique du Médicament, UMR 7175 CNRS-ULP, Université Louis Pasteur-Strasbourg I, 74 route du Rhin, B.P. 24, F-67400 Illkirch, France*
[d] *Centro de Investigaciones Biológicas, CSIC, Ramiro de Maeztu 9, E-28040 Madrid, Spain*

Received 9 May 2008; accepted 20 May 2008

Available online 2 June 2008

Edited by Miguel De la Rosa

Abstract **Mistletoe lectin is a potent biohazard. Lectin activity in the toxic dimer primarily originates from the 2γ-subdomain (Tyr-site) of the B-subunit. Crystallographic information on lectin–sugar complexes is available only at acidic pH, where lectin activity is low. Thus, we mapped ligand-binding properties including comparison to ricin's Tyr-site at neutral pH. Using these results and molecular dynamics simulations, a local conformational change was rendered likely. The obtained structural information is valuable for the design of potent inhibitors.**

Keywords: Agglutinin; Lectin; Mistletoe; Ribosome-inactivating protein; Ricin

1. Introduction

Ribosome-inactivating plant lectins are potent biohazards and also attractive models to study evolutionary routes of intra- and interprotein divergence [1,2]. AB-type toxins combine a toxic A-subunit with the lectin part (B-subunit). Starting from a primordial 40-residues peptide, a series of gene duplications is supposed to have led to the common structural arrangement of the B-chain. It consists of two tandemly arrayed domains (1 and 2) established by four subdomains each (α, β, γ, δ) [3]. Carbohydrate-binding activity is found in the 1α and 2γ subdomains. The potent toxin ricin, the role model of this class, harbours Trp37 in its low-affinity 1α site and Tyr248 in its high-affinity 2γ site [3]. In solution it is monomeric, in contrast to the weakly toxic dimeric agglutinin of the castor bean. The galactoside-specific agglutinin from *Viscum album* L. (VAA; also called viscumin or ML-I) uniquely combines the activities as toxin/agglutinin in one protein [4]. Binding to cells and multivalent glycoproteins is of nM affinity and can engage the 1α domain around Trp38 and the 2γ domain around Tyr249 [5–7]. Because dimer formation spatially restricts accessibility to the Trp-site, the Tyr-site is central for glycan binding and toxicity above submicrogram/ml-levels [7].

Of note for structural design of inhibitors, crystals of VAA-sugar complexes had been grown in acidic pH, i.e. pH 3.4 and 2.5 [8,9], a condition detrimental for lectin activity [10]. The concern for pH-dependent local conformational changes in the binding site arises. It is also valid in the case of ricin, which shares this sensitivity toward pH decrease [11]. To address this issue and also enable interprotein comparison, we here present mapping of the ligand-binding properties of VAA's Tyr-site and, assisted by molecular dynamics simulations, develop a structural model of this site at neutral pH.

2. Materials and methods

2.1. Saccharides

The panel of saccharides was established from sources as given in detail previously [12,13].

2.2. Isolation and labelling of VAA

Purification, labelling with a biotin derivative and quality/activity controls were performed as described previously [5,7]. Biotin-labelled VAA was subsequently acetylated with *N*-acetylimidazole, in the absence or presence of 0.1 M lactose, using a 2-fold excess (w/w) of the reagent [5]. Protein concentration was determined by the Lowry assay using concanavalin A (Sigma) as standard [14]. Radioiodination of VAA using IODO-GEN (Pierce Eurochemie) up to a typical specific activity of 15 ± 5 μCi/mg was carried out in the presence of 0.1 M lactose to protect the carbohydrate-binding sites from modification.

2.3. Quantitative binding studies

Plastic microwells were coated with 50 μl of asialofetuin solution for 16 h at 4 °C and binding of ^{125}I-VAA to the wells was assayed essentially as described [12], except that the buffer used was 5 mM sodium phosphate buffer, pH 7.2, 0.2 M NaCl. For binding assays with biotinylated VAA, precoated wells were incubated with 50 μl of lectin solution for 2 h at 20 °C, and the extent of bound lectin was monitored by measuring the amount of streptavidin associated to the wells after incubation for 1 h at 20 °C with 50 μl (15000 cpm) of ^{125}I-streptavidin solution in the same buffer. Streptavidin (Sigma) was iodinated using IODO-GEN.

The affinity of VAA for the tested saccharides was estimated by determining the amount of ^{125}I-lectin bound to wells coated with 50 μg/ml asialofetuin, after incubation at 20 °C with the ^{125}I-lectin solution in the absence or presence of different concentrations of the sugars.

*Corresponding author. Fax: +34 91 564 2431.
E-mail address: d.solis@iqfr.csic.es (D. Solís).

0014-5793/$34.00
doi:10.1016/j.febslet.2008.05.035

2.4. Molecular dynamics (MD) simulations

Crystallographic parameters of the B chain (pdb entry 1oql) were used as starting point to adapt the Tyr-site residues to neutral pH. Crystallographic water molecules were retained, *N*-acetyl-D-glucosamine groups were removed, and hydrogen atoms were added with Sybyl [15]. The Amber 03 force field was used to model the protein, the generalized amber force field for galactose [16]. Partial charges on galactose were calculated with the AM1-BCC method [17], using Antechamber in the AMBER 8 package [18]. Following addition of one chlorine ion, the system was solvated in an orthorhombic box of TIP3P water molecules ($83.1 \times 86.8 \times 68.6$ Å).

Simulations were carried out with the AMBER 8 suite of programs [18]. The particle mesh Ewald method [19] was used to treat long-range electrostatic interactions; a non-bonded cut-off of 10 Å was used for

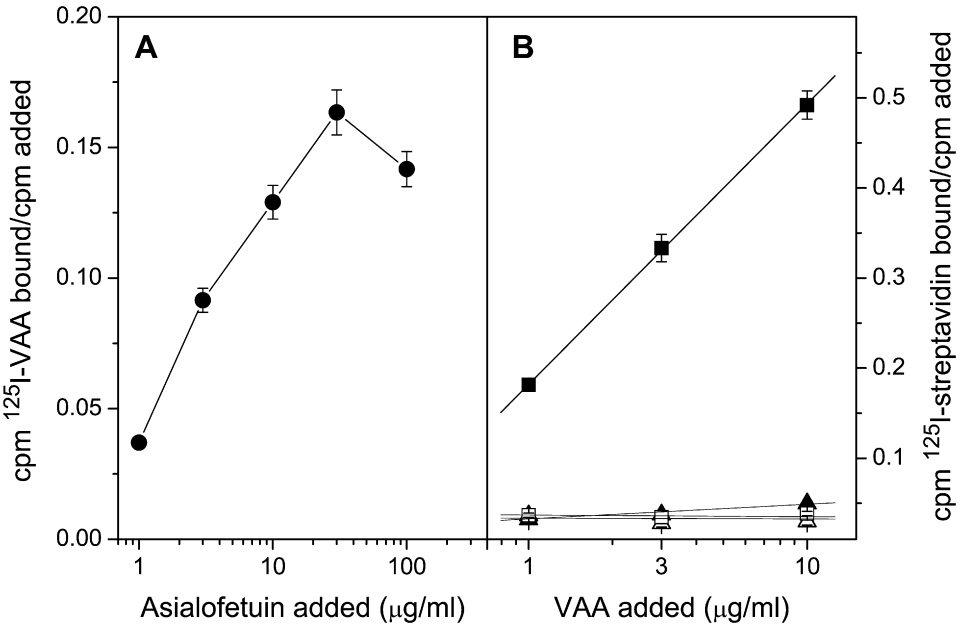

Fig. 1. Binding of VAA to asialofetuin-coated wells. (A) Binding of ^{125}I-VAA to wells coated with asialofetuin solutions of different concentrations was determined as described under Section 2. (B) Biotinylated VAA was treated with *N*-acetylimidazole in the absence (▲, Δ) or presence (■, □) of 0.1 M lactose. Microwell surfaces coated with asialofetuin (100 μg/ml) were then incubated, in the absence (filled symbols) or presence (open symbols) of 0.1 M lactose, with the acetylated biotinylated proteins at three different concentrations. The amount of bound lectin was finally assessed by measuring the binding of ^{125}I-streptavidin to the wells.

Table 1
Apparent association constants for the binding of methyl β-lactoside analogues to VAA

Unit derivatized	Compound	K_a (M^{-1} 10^{-3})		RelativeK_a	
		VAA	Ricin	VAA	Ricin
	Methyl β-lactoside	1.92 ± 0.02	17.8 ± 0.2	1	1
β-D-*Galactopyranose*					
C-2′	2′-Deoxy	0.23 ± 0.02	3.1 ± 0.1	0.12	0.17
	2′-*O*-Methyl	0.28 ± 0.01	13.0 ± 4.9	0.14	0.73
C-3′	3′-Deoxy-3′-fluoro	<0.1	<0.1	<0.05	<0.005
	3′-*O*-Methyl	<0.1	0.50 ± 0.01	<0.05	0.03
C-4′	4′-Deoxy	<0.1	0.33 ± 0.01	<0.05	0.02
	4′-Deoxy-4′-fluoro	<0.1	<0.1	<0.05	<0.005
	4′-*O*-Methyl	<0.1	0.61 ± 0.01	<0.05	0.03
C-6′	6′-Deoxy	0.78 ± 0.4	0.62 ± 0.01	0.4	0.03
	6′-Deoxy-6′-fluoro	0.53 ± 0.01	5.26 ± 0.8	0.3	0.29
	6′-*O*-Methyl	0.50 ± 0.05	10.3 ± 0.3	0.3	0.58
β-D-*Glucopyranose*					
C-1	1-Deoxy	1.50 ± 0.02	18.2 ± 1.0	0.78	1.0
C-2	2-Deoxy	1.15 ± 0.1	16.9 ± 2.6	0.59	0.95
	2-*O*-Methyl	1.1 ± 0.1	10.9 ± 0.7	0.57	0.61
C-3	3-Deoxy	1.8 ± 0.2	37.0 ± 12	0.93	2.1
	3-*O*-Methyl	0.4 ± 0.1	3.2 ± 0.03	0.20	0.18
	3-Deoxy-3-Methyl	0.17 ± 0.01	11.5 ± 0.4	0.1	0.64
	3-Epi	0.34 ± 0.02	2.6 ± 0.1	0.17	0.15
C-6	6-Deoxy	1.30 ± 0.05	8.8 ± 0.3	0.67	0.49
	6-*O*-Methyl	1.1 ± 0.1	7.7 ± 0.3	0.57	0.43

Relative K_a values were calculated taking K_a for methyl β-lactoside as unit. Values for ricin are from reference [11].

van der Waals interactions. A harmonic restraint of 50 kcal mol^{-1} Å^2 was applied on protein residues, with the exception of binding-site residues (within 6.5 Å of galactose) and galactose. The SHAKE algorithm [20] was applied to all bonds involving hydrogen atoms. After minimization, the system was gradually warmed to 300 K in 250 ps; the simulation was then run for 5 ns in the NPT ensemble (T = 300 K; P = 1 atm), with an integration time-step of 2.0 fs.

3. Results

3.1. Binding of VAA to asialofetuin

Tyrosine-radioiodinated VAA bound to asialofetuin-coated wells proportionally to the amount of asialofetuin added to the well (Fig. 1A). Carbohydrate-independent binding in the presence of 0.1 M lactose was always below 1%. The concentration of ^{125}I-labelled lectin in the well was typically 20 μg/ml, neatly above the 3 μg/ml-limit for dimer dissociation becoming appreciable [4]. To attribute binding to the Tyr-site, biotinylated VAA was used. If tyrosine acetylation harms activity and this effect is neutralized by lactose, modification of Tyr249 will account for the loss of activity, as indeed shown in Fig. 1B. Binding of dimeric ^{125}I-VAA to asialofetuin, as does the unlabelled lectin to asialofetuin-Sepharose 4B [7], is thus mediated by the Tyr-sites. They were next subjected to mapping in two stages at neutral pH.

3.2. Carbohydrate-binding profile of the Tyr-sites

First, 20 galactose-based saccharides were tested. The apparent association constants were calculated from the plot of the reciprocal of the lectin fraction bound to the well versus the inhibitor concentration. Most disaccharides only slightly surpassed binding activity of galactose (Supplementary Material, Table). As control, the K_a estimated for the binding of lactose was very close to the value of $(1.1 \pm 0.1) \times 10^3$ M^{-1} previously found by isothermal titration calorimetry at 25 °C and assigned to the Tyr-sites [7].

3.3. Chemical mapping with synthetic methyl β-lactoside derivatives

To dissect the contribution of the hydroxyl groups, we performed a detailed chemical mapping analysis using a series of synthetic deoxy-, fluorodeoxy- and *O*-methyl derivatives of methyl β-lactoside (Table 1). As expected, the most important impact originated from changing groups at the galactose moiety. A large loss in affinity was observed for the derivatives at positions 3′ and 4′ of the galactose unit indicating that these hydroxyls are key groups in the recognition by VAA, as also observed for ricin. At position 2′ there is a weak but significant polar interaction, whereas the hydroxyl group at 6′ is only marginally involved in the binding. Of note, ricin tolerates *N*-acetylation of galactosamine at the 2′-position. These results served as input to infer a pH-dependent conformational change.

3.4. Molecular dynamics simulations

In the crystal structures of VAA in complex with galactose and lactose at acid pH [8,9], the strongest interactions at the Tyr-site involve the hydroxyl groups at positions 3′ and 4′, but no involvement of HO-2′ is visible. To reconcile experimental with structural data, MD simulations were run at neutral pH. In the crystal structure, the side chain of Lys254 is fully oriented towards the solvent (Fig. 2A). After a simulation time of 500 ps, folding of Lys254 towards galactose was observed and a water molecule, W X, was found to mediate the interaction between the C-2 hydroxyl of galactose and the N$^{\zeta}$ group of lysine (Fig. 2B). The vicinity of Lys254 to position 2 of the galactose ring can explain why bulky substituents at this position, as in 2′-*O*-methyl β-lactoside and, more significantly, *N*-acetylgalactosamine, will not enter easily the Tyr-site.

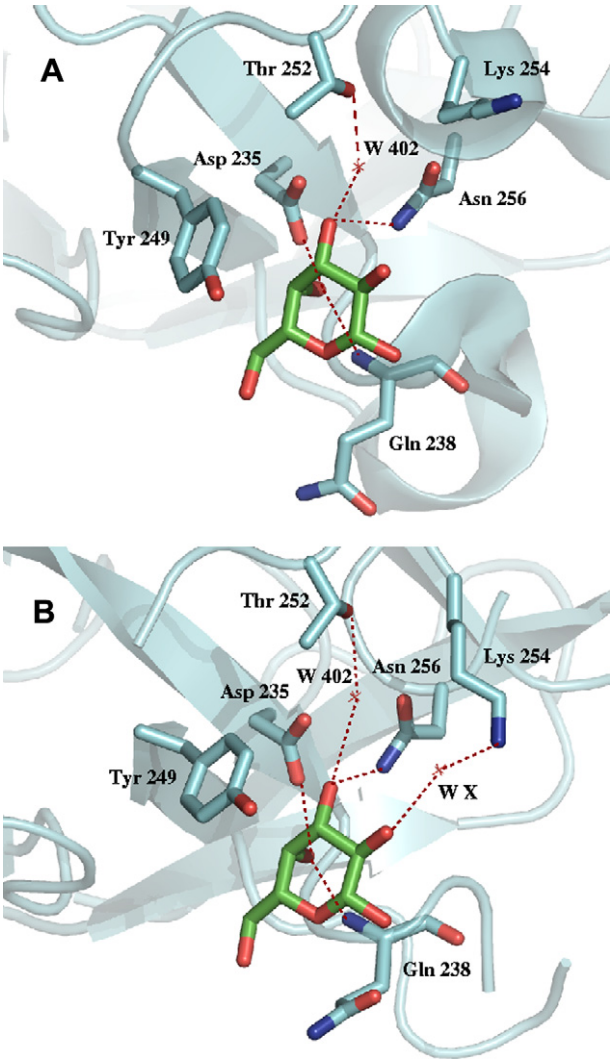

Fig. 2. pH Dependence of the mode of binding of galactose to the Tyr-site of VAA. (A) Binding mode in the crystal structure of the VAA-galactose complex (pdb 1oql) and (B) after a MD simulation at neutral pH. Galactose is shown in green, protein residues in cyan and hydrogen bonds as dotted red lines.

4. Discussion

The results presented here reveal pH-dependent conformational changes and highlight differences in the mode of binding at the Tyr-sites of VAA and ricin. The presented interaction profiles of ligands with substitutions at positions 2′ and 6′ of galactose mainly contribute to explain this disparity, manifested also on the level of cells [21]. The illustrated

pH-dependent change in VAA provides a structural basis for excluding bulky substituents at the 2′-position. Looking at the involvement of HO-6′, it is strongly dependent on the pH in ricin, its role diminishing at acidic pH. In the ricin-lactose complex, crystallized at pH 4.75 [3,22], the C-6′ hydroxyl makes no contacts with the protein. At neutral pH, however, the formation of a salt bridge between Arg236 and Glu199 favours the establishment of a H-bond between N^E (Arg236) and the 6′-hydroxyl group. MD runs revealed the presence of the contacts but they were not stable throughout the simulation, as similarly reported recently [23]. In VAA's Tyr-site, Arg236 and Glu199 are replaced by Ala and Ser, respectively, precluding such a pH-dependent switch for VAA, which tolerates α2,6-sialylation well compared to ricin [24,25]. On the grounds of minor effects of extension to disaccharides in most cases in solid-phase and cell assays [10,26], the noted change at the OH-2′ position of galactose can thus account for modulating ligand affinity at this level of structural complexity.

In summary, the chemical mapping delineates alterations in interaction profiles between VAA and ricin and gives reason to postulate a local pH-dependent conformational change for VAA inferred by modelling. Its detection will optimize design of potent inhibitors, the described strategy being valuable beyond this special protein.

Acknowledgement: This work was supported by DGICYT (BQU2003-03550-C03-03 and BFU2006-10288/BMC), the research initiative LMUexcellent and an EC Marie Curie Research Training Network Grant (Contract No. MRTN-CT-2005-019561).

Appendix A. Supplementary material

Supplementary data associated with this article can be found, in the online version, at doi:10.1016/j.febslet.2008.05.035.

References

[1] Rüdiger, H. and Gabius, H.-J. (2001) Plant lectins: occurrence, biochemistry, functions and applications. Glycoconjugate J. 18, 589–613.
[2] Stirpe, F. (2004) Ribosome-inactivating proteins. Toxicon 44, 371–383.
[3] Rutenber, E. and Robertus, J.D. (1991) Structure of ricin B-chain at 2.5 Å solution. Proteins 10, 260–269.
[4] Jiménez, M., Sáiz, J.L., André, S., Gabius, H.-J. and Solís, D. (2005) Monomer/dimer equilibrium of the AB-type lectin from mistletoe enables combination of toxin/agglutinin activities in one protein: analysis of native and citraconylated proteins by ultracentrifugation/gel filtration and cell biological consequences of dimer destabilization. Glycobiology 15, 1386–1395.
[5] Gabius, H.-J., Walzel, H., Joshi, S.S., Kruip, J., Kojima, S., Gerke, V., Kratzin, H. and Gabius, S. (1992) The immunomodulatory β-galactoside-specific lectin from mistletoe: partial sequence analysis, cell and tissue binding and impact on intracellular biosignaling of monocytic leukemia cells. Anticancer Res. 12, 669–676.
[6] André, S., Kojima, S., Gundel, G., Russwurm, R., Schratt, X., Unverzagt, C. and Gabius, H.-J. (2006) Branching mode in complex-type triantennary *N*-glycans as regulatory element of their ligand properties. Biochim. Biophys. Acta 1760, 768–782.
[7] Jiménez, M., André, S., Siebert, H.-C., Gabius, H.-J. and Solís, D. (2006) AB-type lectin (toxin/agglutinin) from mistletoe: differences in affinity of the two galactoside-binding Trp/Tyr-sites and regulation of their functionality by monomer/dimer equilibrium. Glycobiology 16, 926–937.
[8] Niwa, H., Tonevitsky, A.G., Agapov, I.I., Saward, S., Pfüller, U. and Palmer, R.A. (2003) Crystal structure at 3 Å of mistletoe lectin I, a dimeric type-II ribosome-inactivating protein, complexed with galactose. Eur. J. Biochem. 270, 2739–2749.
[9] Mikeska, R., Wacker, R., Arni, R., Singh, T.P., Mikhailov, A., Gabdoulkhakov, A., Voelter, W. and Betzel, C. (2005) Mistletoe lectin I in complex with galactose and lactose reveals distinct sugar-binding properties. Acta Crystallogr. F61, 17–25.
[10] Lee, R.T., Gabius, H.-J. and Lee, Y.C. (1992) Ligand-binding characteristics of the major mistletoe lectin. J. Biol. Chem. 267, 23722–23727.
[11] Solís, D., Fernández, P., Díaz-Mauriño, T., Jiménez-Barbero, J. and Martín-Lomas, M. (1993) Hydrogen-bonding pattern of methyl β-lactoside binding to the *Ricinus communis* lectins. Eur. J. Biochem. 214, 677–683.
[12] Solís, D., Jiménez-Barbero, J., Martín-Lomas, M. and Díaz-Mauriño, T. (1994) Probing hydrogen-bonding interactions of bovine heart galectin-1 and methyl β-lactoside by use of engineered ligands. Eur. J. Biochem. 223, 107–114.
[13] Alonso-Plaza, J.M., Canales, M.A., Jiménez, M., Roldán, J.L., García-Herrero, A., Iturrino, L., Asensio, J.L., Cañada, F.J., Romero, A., Siebert, H.-C., André, S., Solís, D., Gabius, H.-J. and Jiménez-Barbero, J. (2001) NMR investigations of protein-carbohydrate interactions: insights into the topology of the bound conformation of a lactose isomer and β-galactosyl xyloses to mistletoe lectin and galectin-1. Biochim. Biophys. Acta 1568, 225–236.
[14] Jiménez, M., André, S., Gabius, H.-J. and Solís, D. (2000) Calibration of colorimetric protein assays for quantitation of plant AB toxins. Anal. Biochem. 284, 418–420.
[15] SYBYL 7.1, Tripos Inc., 1699 South Hanley Rd., St. Louis, Missouri 63144, USA.
[16] Wang, J., Wolf, R.M., Caldwell, J.W., Kollman, P.A. and Case, D.A. (2004) Development and testing of a general amber force field. J. Comput. Chem. 25, 1157–1174.
[17] Jakalian, A., David, B.J. and Bayly, C.I. (2002) Fast, efficient generation of high-quality atomic charges. AM1-BCC model: II. Parameterization and validation. J. Comput. Chem. 23, 1623–1641.
[18] Case, D.A., Darden, T.A., Cheatham III., T.E., Simmerling, C.L., Wang, J., Duke, R.E., Luo, R., Merz, K.M., Wang, B., Pearlman, D.A., Crowley, M., Brozell, S., Tsui, V., Gohlke, H., Mongan, J., Homak, V., Cui, G., Beroza, P., Schafmeister, C., Caldwell, J.W., Ross, W.S. and Kollman, P.A. (2004) AMBER 8, University of California, San Francisco.
[19] Essmann, U., Perera, L., Berkowitz, M.L., Darden, T., Lee, H. and Pedersen, L.G. (1995) A smooth particle mesh Ewald method. J. Chem. Phys. 103, 8577–8593.
[20] Ryckaert, J.P., Ciccotti, G. and Berendsdeb, H.J.C. (1977) Numerical integration of the cartesian equations of motion of a system with constraints: molecular dynamics of *n*-alkanes. J. Comput. Phys. 23, 327–341.
[21] Moisenovich, M., Tonevitsky, A.G., Agapov, I.I., Niwa, H., Schewe, H. and Bereiter-Hahn, J. (2002) Differences in endocytosis and intracellular sorting of ricin and viscumin in 3T3 cells. Eur. J. Cell Biol. 81, 529–538.
[22] Villafranca, J.E. and Robertus, J.D. (1977) Crystallographic study of the anti-tumor protein ricin. J. Mol. Biol. 116, 331–335.
[23] Ganguly, D. and Mukhopadhyay, C. (2006) Binding diversity of the two binding sites of ricin B lectin. Biopolymers 83, 83–94.
[24] Galanina, O.E., Kaltner, H., Khraltsova, L.S., Bovin, N.V. and Gabius, H.-J. (1997) Further refinement of the description of the ligand-binding characteristic for the galactose-binding mistletoe lectin, a plant agglutinin with immunomodulatory potency. J. Mol. Recogn. 10, 139–147.
[25] Baenziger, J.U. and Fiete, D. (1979) Structural determinants of *Ricinus communis* agglutinin and toxin specificity for oligosaccharides. J. Biol. Chem. 254, 9795–9799.
[26] André, S., Pei, Z., Siebert, H.-C., Ramström, O. and Gabius, H.-J. (2006) Glycosyldisulfides from dynamic combinatorial libraries as *O*-glycoside mimetics for plant and endogenous lectins: their reactivities in solid-phase and cell assays and conformational analysis by molecular dynamics simulations. Bioorg. Med. Chem. 14, 6314–6326.